Electronic properties of GaAs - AlAs Fibonacci superlattices

1997 J. Phys.: Condens. Matter 9 8031

(http://iopscience.iop.org/0953-8984/9/38/009)

J. Phys.: Condens. Matter **9** (1997) 8031–8039. Printed in the UK PII: S0953-8984(97)85032-1

Electronic properties of GaAs–AlAs Fibonacci superlattices

J Arriaga† and V R Velasco‡

† Instituto de Física Luis Rivera Terrazas, Universidad Autónoma de Puebla, Apartado Postal J-48, 72570 Puebla, Pue., Mexico

‡ Instituto de Ciencia de Materiales, CSIC, Cantoblanco, 28049 Madrid, Spain

Received 10 June 1997

Abstract. We study the electronic band structure and the local density of states of different GaAs–AlAs Fibonacci superlattices grown along the [001] direction. We use an empirical tight-binding Hamiltonian including spin–orbit coupling together with the surface Green function matching method. We have analysed second-to-fifth-generation superlattices with different generating layer thicknesses. A selective localization of the local density of states in the thickest GaAs slabs is found for both the highest valence and lowest conduction band states in all of the cases considered in our study.

1. Introduction

In the last few years much attention has been paid to studies of the physical properties of solids with long-range order, lacking translational symmetry [1–9], induced by the fabrication of aperiodic low-dimensional systems [1, 2] and the discovery of quasicrystals [3, 4]. These aperiodic systems, whose structural order is described by means of deterministic sequences, can be considered as an intermediate case between periodic and disordered one-dimensional solids, and they exhibit rather exotic electronic properties not shared by crystalline and amorphous solids. Among several quasiperiodic models, the Fibonacci system, which is a linear lattice constructed recursively, is the one-dimensional version of the quasicrystals, and it has been the subject of intensive theoretical studies as a model of the quasicrystals. The Fibonacci system has been investigated mainly in the single-band tight-binding limit. Two special cases are usually studied. The first one considers all of the hopping-matrix elements $V_{ij} = V$ constant and the on-site energies E_i take two values, arranged in a Fibonacci sequence. This model is known as the *on-site* model. The second one has the on-site energies $E_i = E_0$ constant but the hopping-matrix elements V_{ij} take two values, arranged in a Fibonacci sequence. This model is known as the *transfer* model. It is found in both models that the energy spectrum is self-similar, and the energy band divides into three subbands, each of which further divides into three and so on [10–14], thus creating a singular continuous spectrum which in the infinite limit reduces to a Cantor-set spectrum with dense energy gaps everywhere [15–18]. A more realistic study was done [19] by using a semiempirical sp^3s^* Hamiltonian [20] and arranging atomic layers of GaAs and AlAs in a Fibonacci sequence. Hirose *et al* calculated the electronic structure up to the 12th generation, which has a total of 144 GaAs and 89 AlAs layers. The GaAs/AlAs system is particularly well suited for these structures, because their parameters can easily be tailored to meet a specific need, and this system has been used to grow Fibonacci superlattices [2, 21]. We shall consider here the effects of the full crystalline structure as in [19] and of

0953-8984/97/388031+09$19.50

the different thicknesses of the constituent layers on the electronic band structure and the localization of the different states of the GaAs/AlAs (001) Fibonacci superlattices.

In section 2 we present the theoretical model and the method of calculation. Results are presented in section 3 and conclusions are presented in section 4.

2. The theoretical model and method

The GaAs/AlAs Fibonacci superlattices are grown by stacking recursively along the z-direction, with two generators, blocks A and B, mapping the mathematical rule in the Fibonacci sequence

$$S_1 = \{\mathrm{A}\} \qquad S_2 = \{\mathrm{AB}\} \qquad S_3 = \{\mathrm{ABA}\} \qquad \cdots \qquad S_n = S_{n-1}S_{n-2} \tag{1}$$

where A consists of $(\mathrm{AlAs})_i/(\mathrm{GaAs})_j$ layers and B of $(\mathrm{AlAs})_i/(\mathrm{GaAs})_l$ layers, which we shall abbreviate as (i, j, l).

The empirical tight-binding (ETB) Hamiltonians [20, 22] are very useful for studying the electronic and optical properties of semiconductor heterostructures. The ETB models include the multiband and band-mixing characteristics together with the crystalline symmetry for the bulk constituent materials, and they can be more useful than the $\boldsymbol{k}\cdot\boldsymbol{p}$ method in the study of the properties of these systems in the complete Brillouin zone. It is also known that self-consistent ETB calculations for semiconductor interfaces [23–25] gave results for the band offset comparable to those obtained within the local density approximation (LDA) [26]. It is then clear that the ETB Hamiltonians are a good choice for studying the electronic properties of Fibonacci superlattices on a more realistic basis, beyond the aspects studied with the *transfer* and *on-site* models. We use an $\mathrm{sp^3s^*}$ ETB Hamiltonian [20] including nearest-neighbour interactions and spin–orbit coupling [27]. The ETB parameters are those employed in [28], and we have used the following energy reference: $E_V(\mathrm{AlAs}) = -0.55$ eV, $E_C(\mathrm{AlAs}) = 1.75$ eV, which corresponds to the AlAs indirect band gap, $E_V(\mathrm{GaAs}) = 0.0$ eV and $E_C(\mathrm{GaAs}) = 1.55$ eV. This band offset is within experimentally accepted values for (001) interfaces [29] and corresponds to a 66/34 band-offset rule [30].

The Fibonacci superlattices involve many inequivalent interfaces. We shall employ a recently developed version of the surface Green function matching (SGFM) method [31], specially adapted to deal with an arbitrary number N of inequivalent interfaces [32]. The method has been fully explained in [32] and will not be repeated here. The eigenvalues are obtained from the peaks in the imaginary part of the trace of the interface projection of the Green function of the matched system $\tilde{\boldsymbol{G}}_S^{-1}$ [32]. A small imaginary part of 10^{-3} eV was added to the real energy variable, which was varied in steps of 0.01 eV, and iterations were carried out until absolute differences between the last iterations of order 10^{-6} eV were obtained. We have found in previous practical calculations that this provides a satisfactorily accurate procedure. The spatial localization was obtained by calculation of the local density of states in the different layers of the Fibonacci superlattice period, which is directly obtained from the Green function of the whole system $\boldsymbol{G}_S$ [32].

3. Results

We have considered different combinations for the A, B blocks, and consequently the (i, j, l) indices quoted above. Our choice has been to find numbers such that $(i + j)/(i + l)$ is very close to the *golden mean* given by $(\sqrt{5} + 1)/2$, although this

requirement is not essential [2, 21]. The (i, j, l) generators considered in our study were $(3, 10, 5)$, $(5, 8, 3)$, $(7, 14, 6)$, $(8, 13, 5)$ and $(10, 11, 3)$, ranging from the second to the fifth generation, and ranging from *four* to *sixteen* inequivalent interfaces. In this way it will be possible to study the influence of the relative thicknesses of the constituent materials on the properties of the Fibonacci superlattices.

The band structures of the different superlattices exhibit a similar appearance to that shown in [19], the only difference being the lifting of the degeneracy in the heavy-hole band due to the inclusion of the spin–orbit coupling, and they will not be shown here. This behaviour can be seen in a different way by looking at the density of states at different symmetry points.

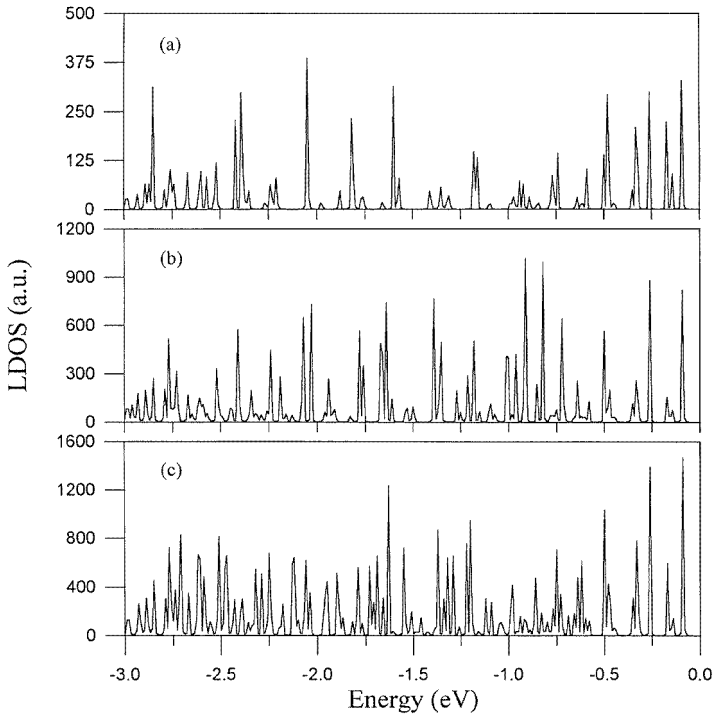

Figure 1. The LDOS summed over a superlattice period, in arbitrary units, for the valence bands at the Γ point of a $(5, 8, 3)$ Fibonacci superlattice. (a) Third generation; (b) fourth generation; (c) fifth generation.

Figure 1 gives the local density of states (LDOS), summed over a superlattice period, in arbitrary units, for the valence bands at the Γ point, for the third, fourth and fifth generations of a $(5, 8, 3)$ Fibonacci superlattice. It can be seen that the range -0.5 eV $\leqslant E \leqslant 0$ eV exhibits the same structure for the different generations, but for the lower energies the number of states increases with increasing number of generations, and the trifurcation of the heavy holes can be seen.

Figure 2 gives the same information for the conduction band states. It can be seen that the behaviour of the LDOS in the range 1.6 eV $\leqslant E \leqslant 2$ eV is very similar for the different generations. For higher energies, up to 3 eV, the number of states increases with increasing number of generations, but no trifurcation is seen, and no Fibonacci structure appears. In that energy region the conduction states have no s character, like in the lower-energy region,

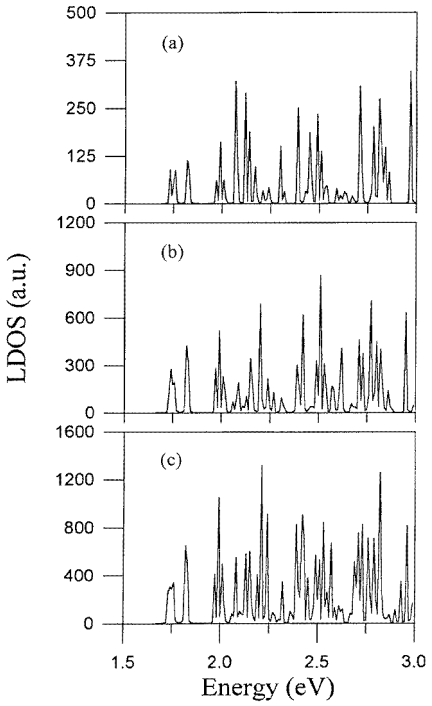

Figure 2. As figure 1, but for the conduction band states of a $(5, 8, 3)$ Fibonacci superlattice.

but they have s, p and s* contributions, coming from the AlAs X point. This band mixing destroys the Fibonacci structure in that region.

Figure 3 gives the LDOS summed over a superlattice period, in arbitrary units, for the valence bands at the X point corresponding to the third, fourth and fifth generations of a $(5, 8, 3)$ Fibonacci superlattice. It can be seen that the LDOS has the same behaviour in the different generations, and that only a small number of states exist, as opposed to the case of the Γ point in figure 1. In this case no Fibonacci structure exists. This high degeneracy at the X point is induced by a strong mixing of the different states, and the Fibonacci structure is destroyed, independently of how high the Fibonacci generation number is.

Figure 4 presents the same information for the conduction band states. It is easy to see that we have a repetition of the behaviour seen in figure 3. A high degree of degeneracy of the conduction states is evident, as compared with figure 2, and no Fibonacci structure survives to the strong mixing of the different states.

We have seen that the Fibonacci structure is only found at some points of the superlattice Brillouin zone, mainly in the vicinity of the Γ point, and for some energy ranges. This can easily be understood if we take into account that our model includes different on-site energies and hopping parameters for the different orbitals, the valence band offset and the three-dimensional crystal geometry, and the Fibonacci sequence acts on all of these items. It is then clear that the clear-cut predictions of the *on-site* and *transfer* models must be blurred, at least, or even destroyed in our case. It is easy to understand that those states having no strong mixing of the different orbitals will be more suitable for providing evidence of the Fibonacci structure, as shown before.

We shall pass on to studying now the spatial localization of the lowest conduction band

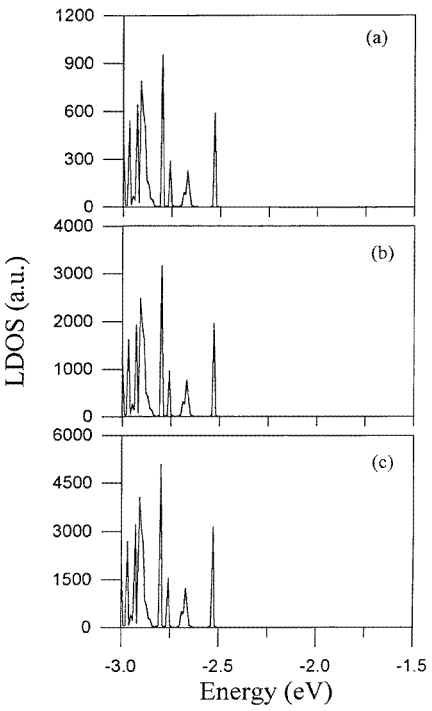

Figure 3. As figure 1, but for the valence band states at the X point of a $(5, 8, 3)$ Fibonacci superlattice.

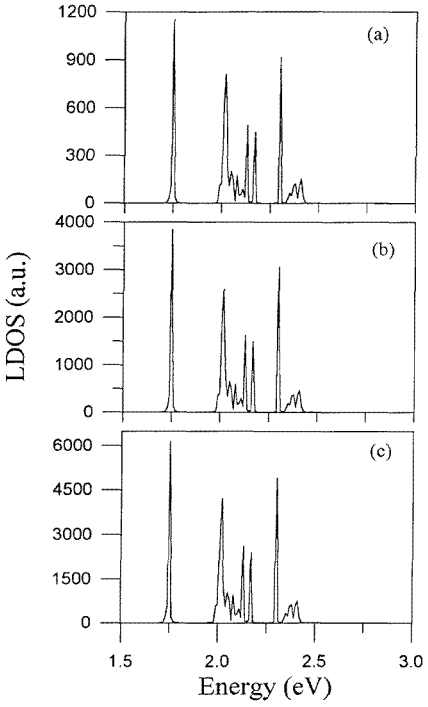

Figure 4. As figure 3, but for the conduction band states of a $(5, 8, 3)$ Fibonacci superlattice.

and highest valence band states at the superlattice Γ point, which are among those exhibiting the Fibonacci structure as discussed before. We shall consider here different generators to see the influence of the relative thicknesses of the constituent slabs on the spatial localization of the different states.

In all of the cases studied we have found that they concentrate in the thickest GaAs slabs in the superlattices, although some spectral strength can be found in the narrowest GaAs slabs and the intervening AlAs slabs in some cases. Some additional features of the spectral strength can be found, and they will be illustrated now.

Figure 5 gives the local spectral strength, in arbitrary units, corresponding to the two highest valence band states of a fourth-generation $(8, 13, 5)$ superlattice versus the atomic layers in the period of the superlattice. The energies of these states are -0.04 eV and -0.09 eV, respectively. We see the localization in the GaAs slab having 13 monolayers. It is also clear that the behaviour is different in the two cases. In the first case the spectral strength is the same in the three thickest GaAs slabs, while there is a clear difference in the lower state.

In figure 6 we present the same information for the fourth generation of a $(7, 14, 6)$ Fibonacci superlattice. The sum of AlAs and GaAs layers in the generating blocks of this superlattice is the same as that in the $(8, 13, 5)$ one, and the thicknesses of the constituent slabs differ by one monolayer only. The situation is analogous to that of figure 5, although the behaviour of the spectral strength corresponding to the lower state is the reverse of that shown in figure 5. The energy values of the states considered in figure 6 are -0.04 eV and -0.08 eV, respectively.

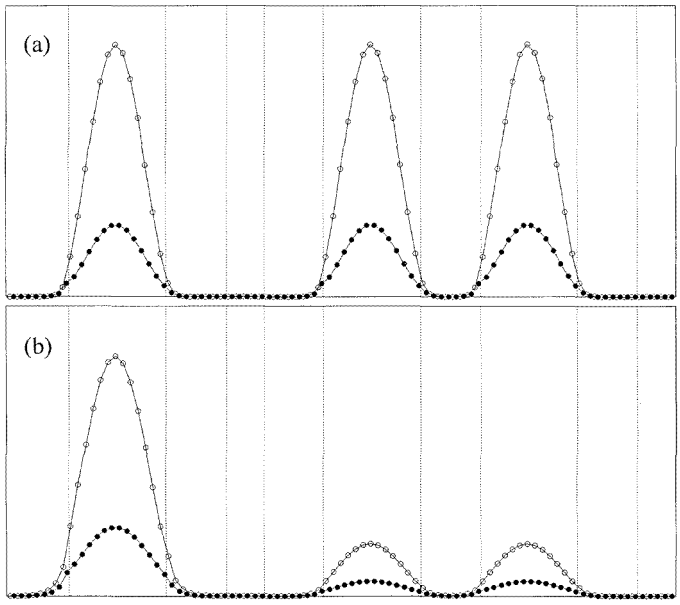

Figure 5. The distribution of the LDOS, in arbitrary units, of the two highest valence band states at the Γ point in the different layers of a (8, 13, 5) fourth-generation Fibonacci superlattice. (a) $E = -0.04$ eV; (b) $E = -0.09$ eV. (•, cations; ○, anions.)

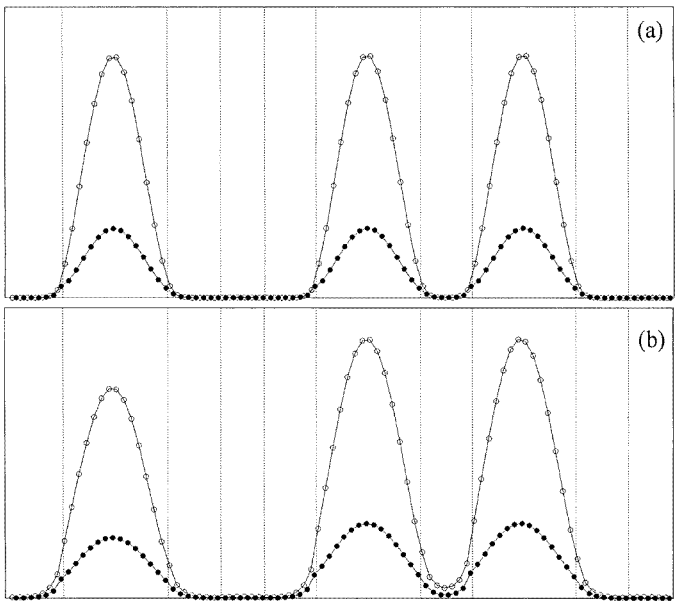

Figure 6. As figure 5, but for a (7, 14, 6) fourth-generation Fibonacci superlattice. (a) $E = -0.04$ eV; (b) $E = -0.08$ eV.

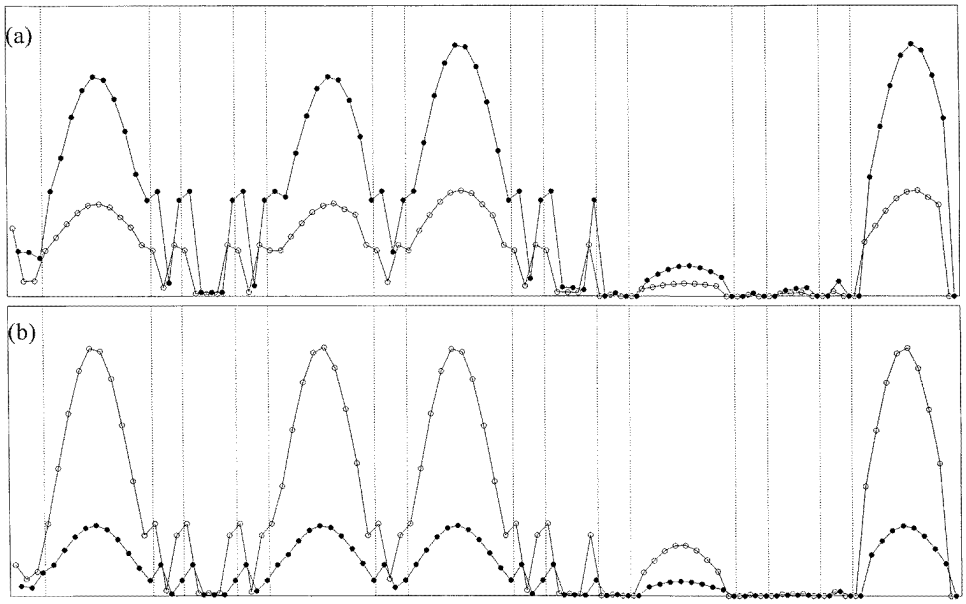

Figure 7. The distribution of the LDOS, in arbitrary units, of (a) the lowest conduction band state ($E = 1.68$ eV) and (b) the highest valence band state ($E = -0.06$ eV) at the Γ point in the different layers of a $(3, 10, 5)$ fifth-generation Fibonacci superlattice. (•, cations; ○, anions.)

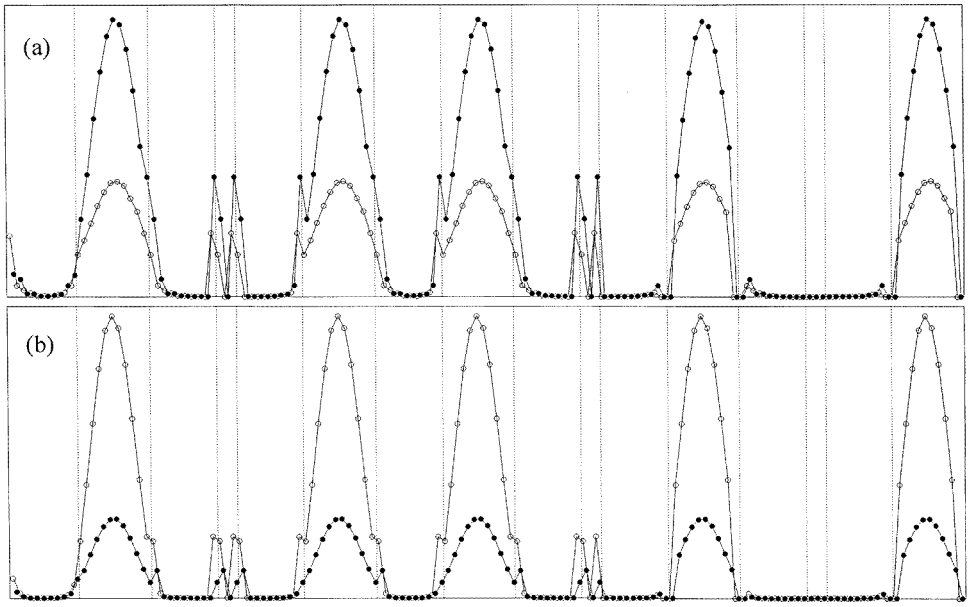

Figure 8. As figure 7, but for a $(10, 11, 3)$ fifth-generation Fibonacci superlattice. (a) $E = 1.68$ eV and (b) $E = -0.06$ eV.

In figure 7 we present the local spectral strength, in arbitrary units, corresponding to the lowest conduction band and highest valence band states of the fifth generation of a $(3, 10, 5)$ Fibonacci superlattice. The energies of these states are 1.68 eV and -0.06 eV, respectively. The same behaviour of the spectral strength is evident for the two states. A completely analogous behaviour is observed for the $(5, 8, 3)$ superlattice which corresponds to the same $(i + j)/(i + l)$ value.

Figure 8 shows the same information for the fifth generation of a $(10, 11, 3)$ Fibonacci superlattice. The energies of the corresponding states are also 1.68 eV and -0.06 eV, respectively. The behaviour of the spectral strength is the same for the two states, but it shows a difference as compared to figure 7. In figure 8 the spectral strength is concentrated in the same way in all of the 11-monolayer GaAs slabs, while in figure 7 it is clear that one of the 10-monolayer GaAs slabs shows a clear reduction in the spectral strength contained there. The energy values of these states are very close to those of GaAs quantum wells with 10 and 11 monolayers [33], and quite different from those corresponding to GaAs quantum wells of 3 and 5 monolayers [33], which are the other GaAs thicknesses entering the superlattices under consideration. The predominant localization in the thickest GaAs slabs is then understandable.

We have seen that there are some different cases related to the different thicknesses of the constituent slabs, although the main conclusion is the selective localization in the thickest GaAs slabs of the lowest conduction and highest valence band states in the different Fibonacci superlattices considered here.

4. Conclusions

We have studied the second to the fifth generation of different (001) GaAs/AlAs Fibonacci superlattices, by means of an ETB sp^3s^* Hamiltonian and the SGFM method. We have found that the Fibonacci structure can only be observed for some energy ranges and for wavevectors in the vicinity of the superlattice Γ point. The states showing the Fibonacci structure do not have a strong mixing of the different orbital components, and therefore are similar to those described by the *on-site* and *transfer* one-dimensional models. We have also seen that the lower conduction and higher valence band states show a selective spatial localization in the thickest GaAs slabs forming the superlattice, although some particular situations associated with the relative thicknesses of the slabs forming the superlattices can be found.

Acknowledgments

This work was partially supported by the European Community under Grant No CI1*-CT94-0046, the CONACYT (Mexico) under Grant No E9403-4035, and the Dirección General de Investigación Científica y Técnica (Spain) under Grant No PB93-1251.

References

[1] Levine D and Steinhardt P J 1984 *Phys. Rev. Lett.* **53** 2477
[2] Merlin R, Bajema K, Clarke R, Juang F-Y and Bhattacharya P K 1985 *Phys. Rev. Lett.* **55** 1768
[3] Shechtman D, Blech I, Gratias D and Cahn J W 1984 *Phys. Rev. Lett.* **53** 1951
[4] Goldman A I and Kelton R F 1993 *Rev. Mod. Phys.* **65** 213
[5] Eric S-R and Das Sarma S 1988 *Phys. Rev.* B **37** 4007

[6] Yamaguchi A A, Saiki T, Tada T, Ninomiya T, Misawa K and Kobayashi T 1993 *Solid State Commun.* **85** 223
[7] Tuet D, Potemski M, Wang Y Y, Maan J C, Tapfer L and Ploog K 1991 *Phys. Rev. Lett.* **66** 2128
[8] Munzar D, Bročáev L, Humlíček J and Ploog K 1994 *J. Phys.: Condens. Matter* **6** 4107
[9] Domínguez-Adame F and Maciá E 1996 *Phys. Rev.* B **53** 13 921
[10] Niu Q and Nori F 1986 *Phys. Rev. Lett.* **57** 2057
[11] Niu Q and Nori F 1990 *Phys. Rev.* B **42** 10 329
[12] Liu Y and Riklund R 1987 *Phys. Rev.* B **35** 6034
[13] Fujita M and Machida K 1986 *Solid State Commun.* **59** 61
[14] Ninomiya T 1986 *J. Phys. Soc. Japan* **55** 3709
[15] Kohmoto M, Kadanoff L P and Tang C 1983 *Phys. Rev. Lett.* **50** 1870
[16] Ostlund S, Pandit R, Rand D, Schnellnhuber H J and Siggia E D 1983 *Phys. Rev. Lett.* **50** 1873
[17] Kohmoto M and Benavar J R 1986 *Phys. Rev.* B **34** 563
[18] Kohmoto M, Sutherland B and Tang C 1987 *Phys. Rev.* B **35** 1020
[19] Hirose K, Ko D Y K and Kamimura H 1992 *J. Phys.: Condens. Matter* **4** 5947
[20] Vogl P, Hjalmarson H P and Dow J D 1983 *J. Phys. Chem. Solids* **44** 365
[21] Todd J, Merlin R, Clarke R, Mohanty K M and Axe J D 1986 *Phys. Rev. Lett.* **57** 1157
[22] Slater J C and Koster G F 1954 *Phys. Rev.* **94** 1498
[23] Muñoz A, Sánchez-Dehesa J and Flores F 1987 *Phys. Rev.* B **35** 6468
[24] Haussy B, Priester C, Allan G and Lannoo M 1987 *Phys. Rev.* B **36** 1105
[25] Flores F, Durán J C and Muñoz A 1987 *Phys. Scr.* T **19** 102
[26] Van de Walle C G and Martin R M 1986 *J. Vac. Sci. Technol.* B **4** 1055
[27] Chadi D J 1977 *Phys. Rev.* B **16** 790
[28] Contreras-Solorio D A, Velasco V R and García-Moliner F 1993 *Phys. Rev.* B **48** 12 319
[29] Fu Y and Chao K A 1991 *Phys. Rev.* B **43** 4119
[30] Kopf R T, Herman M H, Schnoes M L and Colvard C 1993 *J. Vac. Sci. Technol.* B **11** 813
[31] García-Moliner F and Velasco V R 1992 *Theory of Single and Multiple Interfaces* (Singapore: World Scientific)
[32] Fernández-Alvarez L, Monsivais G, Vlaev S and Velasco V R 1996 *Surf. Sci.* **369** 367
[33] Velasco V R and García-Moliner F 1994 *Prog. Surf. Sci.* **46** 211